

Portable Femtosecond Laser Machine Delivered to HEAF

Under the support of DOE's Stockpile Stewardship Program and DOD's Office of Munitions, we recently developed and delivered a compact, portable femtosecond laser system to the Defense and Nuclear Technologies Program (D&NT) to be used in the High Explosives Application Facility (HEAF) for precision-machining of high explosives, other energetic materials, and various weapons components.



Recent material processing experiments using short-pulse lasers have clearly demonstrated that the femtosecond laser pulses can cut materials with high precision and negligible transfer of energy (both thermal and shock) to the bulk of the object. Small quantity of high explosives (200mg pellets made of PETN, HMX, TATB or TNT, etc.) were successfully machined using a pulsed laser with 120-fs pulse duration and showed no detonation or deflagration (see Figure 1a). As a demonstration of the sensitivity to pulse-duration we also tried cutting with 500-ps laser pulses. Bulk heating is anticipated in this case because the pulse-duration is significantly longer than the time needed for transferring energy between electrons and phonons which is about 10-ps in dielectrics. As shown in Figure 1b, the heat deposited by the 500-ps pulses fueled an intense burn of the HE pellet.



HE pellet cut with fs lasers pulses



HE pellet cut with ps pulses

The HEAF laser-cutting machine is very compact and fully automated, and can be operated by personnel with little laser expertise. The machine is mounted on a portable 4'x10' optical table which can be rolled inside the HEAF facility for various scale of experiments. The overall system consists of a short-pulse Ti: sapphire laser, beam positioning and power control equipment. It has an average output of 5 W (1.4 mJ @ 3.5 kHz, 120 fs pulse-duration), with a capability to increase to 20-25 W when additional power-amplifiers and pump lasers are installed. Instead of an arc-lamp-pumped pump laser as in the system delivered to Y12, the system incorporates a frequency-doubled, diode-pumped solid-state laser as pump source. Diode pumping improves the machine maintenance interval from every three weeks (required for the lamp-pumped systems) to over one year. Activation of the laser system in HEAF is currently underway.

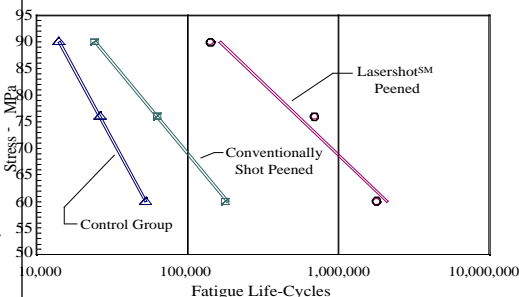
LasershotSM Peening Improves Service Life of Metal Parts

In a collaborative effort with the Metal Improvement Co. Inc, we are evaluating the effectiveness of LasershotSM peening in extending the service life of metal components for industrial and government application. Using a kilowatt-class, 100 J/pulse, Nd:doped glass laser, we were able to rapidly treat the surfaces of metal components and induce deep compressive stress to significantly extend their service life.

By optimizing the process parameters such as laser pulse duration (10-to-30 ns), fluence, intensity (100-to-300 J/cm²) and number of treatment pulses, we have treated a broad range of materials including aluminum, titanium, nickel and steel-based alloys. Since fatigue cracks on metal components typically develop at the surface; deep compressive stress can prevent their initiation and growth and consequently improve component lifetime. Test results have shown deep compressive stress on the work piece extending to depths of 0.1 inches. As shown in the figure below, recent fatigue tests on 2024 T3 aluminum, under various stress load conditions, show more than 50 times improvement in fatigue lifetime for structural aluminum test plates when compared to conventional shot peening.

LasershotSM peening could be used to extend the service lifetime of many critical parts from jet-engine fan blades, F-16 bulkheads to hip joints. One application recently identified for DOE's Civilian Radioactive Waste Management System (CRWMS) Program is to improve the service lifetime of metal canisters, designed for long-term disposal of high-level radioactive waste (generated by commercial nuclear power plants and government reactors) potentially at Yucca Mountain in Nevada, which will be discussed in a future Update issue.

Comparison - Laser peening versus conventional shot peening on Laser drilled holes in aluminum



Fatigue Life-Cycle Measured in Aluminum



Falcon Laser Making Progress Toward Integration with Linac

With the widespread development of high-peak-power lasers based on chirped pulse amplification, the potential for high-brightness, laser-based, ultrafast sources of x rays now exists. The development of these sources is very attractive since the production of hard x rays ($E > 10$ keV) with a pulse width below 100 fs will make possible unique experiments studying the ultrafast dynamics of matter. Such experiments include watching the motion of atoms in a material or chemical reaction upon laser excitation.

To make such experiments possible, a unique x-ray source is being developed at Lawrence Livermore National Laboratory. This source is based on the integration of the Falcon, a multiterawatt femtosecond laser, with a high-energy (100 MeV) electron linear accelerator (linac). Through Thomson scattering of laser photons off a tightly focused low-emittance beam of relativistic electrons, bursts of tunable hard x rays with pulse duration less than 100 fs will be produced. Doing this entails crossing the femtosecond laser pulse with a 1-ps electron bunch, a task that requires state-of-the-art laser-electron beam synchronization. Progress toward this challenging technical goal has been recently achieved at the Falcon laser (shown below).



The Falcon laser is a Ti:sapphire laser based on chirped pulse amplification. It produces 0.5-J pulses of 35-fs duration at 1 Hz and is currently undergoing an upgrade to the 4 J per pulse level. Transport of these pulses to the B194 linac is under way. A major step toward the integration of Falcon with the linac was recently demonstrated. Photoelectrons produced by seed pulses from the Falcon laser were accelerated in an RF photo-gun (developed by a collaboration with the Engineering Directorate) to 5 MeV (see photo below).

This milestone demonstrates the technical feasibility of the integrated time synchronization and represents a major step toward interacting the Falcon beam with full-energy electron pulses. System integration will continue, with the goal of producing modest-brightness, soft x-ray pulses from the photo-gun electrons by late this spring. Full system integration with the 100-MeV linac, injected with electrons from the photo gun, will commence after this first proof-of-principle demonstration.



Output Irradiance of 1 kW/cm² Delivered by Laser Diode Array Cooled by Monolithic Heatsink

For commercial and military applications, there is a need for high-performance laser diode arrays that can be manufactured cost-effectively.

Historically, high-average-power heatsinks have been complex to produce



because of the fabrication processes that are needed to provide separate cooling for each laser bar. Alternatively, available monolithic heatsink designs that share a common cooling backplane are simpler, but the thermal performance is not sufficient for many applications.

Our objective is to develop a diode-array that combines the advanced cooling capabilities of discrete heatsinks in a monolithic design. We have recently produced a silicon monolithic microchannel (SiMM) heatsink that can allow up to ten diode bars to be bonded onto a single cooler. The figure above shows a 10-bar diode array mounted on a silicon monolithic microchannel cooler. The thermal impedance of the diode-array package is low ~ 0.35 K/W even at high bar packing density. Because of the low thermal impedance, we can reliably operate the diode array at outputs up to 50 W/bar cw, or 150 W/bar peak at 25% duty factor with a moderate temperature rise at the diode junction. An output irradiance of 1 kW/cm² was demonstrated.

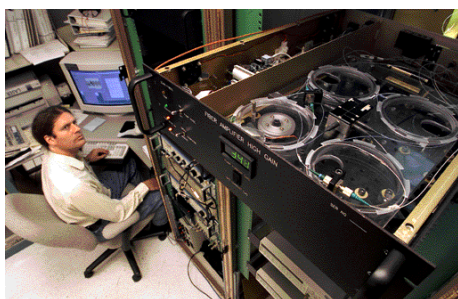
An advantage of the silicon heatsink is that it can be fabricated with lithographic accuracies, such that the diode emission can be collimated to low angular divergence using a single Si-etched lens frame. This packaging approach scales gracefully to large areas and high power, a critical element in diode-pumped solid-state lasers envisioned for the future.

Long-Term Wavelength and Gain Stability Demonstrated by NIF Master Oscillator Components

The master oscillator is one of the most important subsystems in the National Ignition Facility (NIF) because it controls the laser's wavelength, linewidth, pulse shape, and timing. In the master oscillator room (MOR), a single laser pulse is produced, phase-modulated to add bandwidth, and multiplexed into 48 separate beamlines on single-mode, polarizing fiber. Before feeding into the entire NIF laser system, the pulses are amplitude-modulated into high-contrast shaped pulses required for target ignition.

Working with the NIF optics team, we have recently built and tested several of the MOR components including the master oscillator, fiber amplifiers, and amplitude modulator. In a lab designed to simulate environmental conditions of NIF, we measured the stability of the output pulses. Since there are so many active components in the system, each must contribute less than 1% instability to the signal in order to meet NIF requirements. The photo below shows a first article MOR hardware under test. All optical and electronic systems are mounted inside chassis and linked by polarizing fiber cables. The fiber is a custom type produced by 3M, with 5-dB/m differential attenuation between the two polarization axes, and less than 0.03-dB/m loss in the transmitting axis.

The oscillator is a distributed feedback (DFB) fiber laser, operating at 1053 nm and



thermally stabilized to better than ± 1 -pm wavelength stability. It emits about 20 mW CW, which is then acousto-optically chopped to a 100-ns pulse and amplified in double-pass fiber amplifier to 1-W peak power. When feedback becomes stabilized, the power stability is about 0.5%. An electro-optic modulator with >50-dB on/off extinction ratio is used to chop this pulse to 30-ns duration before it is amplified in another type of fiber amplifier with small signal gain of >80 (losses in between limit the output power to less than 30 W peak). Long-term gain stability is <1% over several hours. Large signal pulse saturation tests indicate saturation energy is about 2 μ J, providing us with low pulse distortion.

Ongoing tests in the next few months will include phase modulation, complex pulse shaping, and low-jitter (<12 ps rms) synchronization of shaped pulses, all integrated in a NIF configuration.

Meter-Scale Diffraction Gratings Delivered to Petawatt Laser Facilities around the World

Following on the success of fabricating diffraction gratings used in Lawrence Livermore National Laboratory's (LLNL's) Petawatt laser, we have been actively engaged in manufacturing gratings for large-aperture short-pulse laser systems around the world. End users have not been able to obtain gold-overcoated gratings of sufficient efficiency, efficiency uniformity, stability, wavefront flatness and size, so they have been turning to LLNL to supply them.

During 1999, we have fabricated over 40 large-aperture gratings (with diameter of 150 to 400 mm and 1480 to 1800 line-pairs/mm) through work-for-others contracts with institutes from France, Germany, Great Britain, Japan, and Korea.

We have also made gold-overcoated and ion-beam etched gratings for NASA and other DOE laboratories.

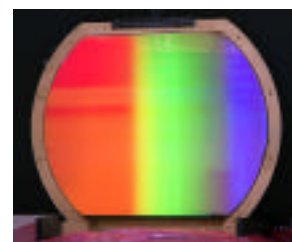
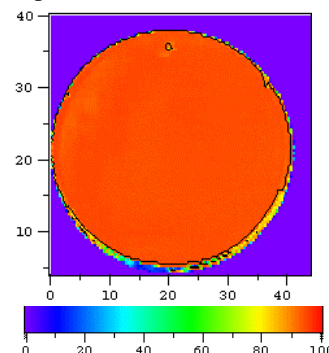


Photo above is one of the meter-scale metallic gratings developed for pulse compression. We have successfully fabricated gold gratings on 94-cm substrates using laser interference lithography. The diffraction efficiency of grating is >96% at the use wavelength and Littrow angle. The damage threshold is greater than 400 mJ/cm² for a 10-ps pulse. The efficiency uniformity of our gratings is also high. Photo below shows the uniformity of diffraction efficiency of a 400-mm-diam grating (1480 lines/mm) measured at 41° incidence angle. Average efficiency over entire part is 93.5%.

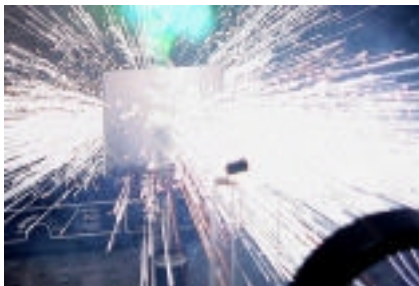


Although we have recently dismantled Nova and lost the facility to do Petawatt-class laser experiments in the U.S., our unique large-aperture grating technology will enable us to revitalize this capability in the future. We are also currently developing all-dielectric gratings using ion-beam etching techniques for a variety of specialized applications.



Modeling of Material Removal by the Heat-Capacity Laser

Under the support of Army Space and Missile Defense Command (SMDC), we are working with Raytheon to evaluate the effectiveness of pulsed solid-state lasers for target interaction, specifically material removal. Using the heat-capacity laser at LLNL, we performed a series of target interaction experiments. Coupons of steel, aluminum and carbon composite were irradiated by the laser beam. During these tests, the energy of the laser was kept at 80 J per pulse, with a pulse duration of 300- to 400-ms at a repetition rate of 10 Hz. Each laser pulse consisted of several relaxation-oscillation spikes with peak irradiance on target near 2×10^7 W/cm². The photos below shows some preliminary results made with the three-slab heat-capacity laser testbed. We were able to penetrate 2.3-mm plates of steel after about 13 laser pulses.



In order to optimize the pulse format for material removal and to guide future target interaction experiments, we are developing numerical models to simulate the material removal process. Using a one-dimensional vaporization-hydrodynamics model, we determined that vaporization was only part of the material removal rate observed in the

Calculated density distribution within the steel, after the pulse. The color scale gives the common logarithm of the density normalized by the solid density. The units are cm (vertically) and microns (horizontally), and the arrow gives the beam radius..

experiments. A majority of the target material appears to be removed by liquid or solid ejection processes.

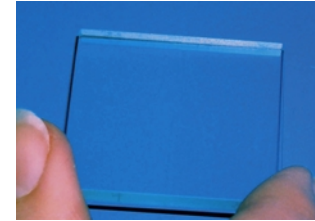
We employed a two-dimensional hydrodynamics code to model both ejection and vaporization. This code makes use of an Arbitrary Lagrangian-Eulerian mesh. It provides a unified description of phenomena within both the target and the blow-off region, which extends several centimeters from the surface. The photo above shows the progressive density depletion within the steel target during the irradiation pulse. Note the steep density gradient near the edge. Typical gas temperature near the target surface reaches 3000 to 4000 K and then cools to 2000 K at the end of the pulse.

We have also calculated the hole depth following the temporal profile of the irradiation pulse. After a threshold, the hole depth appears to increase proportionally with the laser energy absorbed. The final hole depth at the end of the pulse reaches about 175 μ m, consistent with the hole depth achieved experimentally.

Further coupon experiments and detailed numerical modeling are planned. Simulation of the entire experiment requires a sequence of such calculations for each pulse, supplemented by thermal diffusion calculations during the interval between pulses. The continuous buildup of residual heat during successive pulses is anticipated to enhance the overall efficiency of material removal.

(C. Boley)

beam radius



Yb:S-FAP Crystals Being Developed in a 4-x6-cm Size for the Mercury Laser

The Mercury laser is designed to be a 100-J, 10% efficient, 10-Hz laser operating at 1.047 nm. It is based on gas-cooled, diode-pumped crystal laser technology. When completed, it will be the highest energy pulse diode-pumped solid-state laser built to date. One of the critical elements in the Mercury laser development is the growth of high optical quality Yb:S-FAP [Yb³⁺:Sr₅(PO₄)₃F] crystals for the large-aperture gain medium.

We have recently made several technical advances in the crystal growth areas. Yb:S-FAP crystals are grown by using the Czochralski method in which a boule is pulled from a molten mixture of the appropriate-composition starting materials. To minimize optical defects for high-power application, we precisely controlled the growth conditions. For example, an excess amount of SrF₂ was added to the melt to remove the cloudiness commonly observed in crystals associated with incorrect stoichiometry. In addition, crystals were grown along a specific direction to eliminate anomalous optical absorption. Special procedures were also developed to "grow out" grain boundaries that cause unwanted waviness in crystals. Crystal-growth chambers with high thermal stability and controllable temperature gradient were developed to reduce voids (bubbles) in the crystal structure caused by unstable conditions at the crystal/melt interface. With the ability to successfully diffusion-bond Yb:S-FAP crystals together, smaller-diameter boules (2-3 cm) can now be bonded to yield high-optical-quality pieces for full size 4- x 6-cm slabs needed for Mercury.

(K. Schaffers)



Laser Science & Technology

Dr. Howard T. Powell, Program Leader

UCRL-TB-136126-00-05

Construction of the Z/Beamlet: A New, High-Energy, Solid-State Laser System at Sandia National Laboratories

Under the auspices of the Department of Energy's Inertial Confinement Fusion (ICF) Program at Sandia National Laboratories (SNL), we are building a laser backlighter system (the Z/Beamlet) at Sandia's Z facility in Albuquerque, New Mexico. The Z facility employs electrical pulsed power to drive a z-pinch implosion, which efficiently generates x-rays to drive ICF target physics experiments. In recent years, Z has produced up to 2 MJ of x-rays per shot at 15 to 20% conversion efficiency from electrical input energy. Peak x-ray output power from Z reached over 250 TW in 1998.

The new laser backlighter system will provide a powerful new x-ray radiographic diagnostic for quantitative measurements in z-pinch-driven target experiments. In this application, new information would be obtained by recording images and/or spectra of x-ray radiation transmitted through target materials as they evolve during Z-accelerator-driven experiments or shots.

The Z-Backlighter Project involves a team of scientists, engineers, and technicians from both Lawrence Livermore National Laboratory (LLNL) and SNL, and is scheduled for completion by the end of December 2000, with shots to the Z-facility target chamber. Many of the components of the new laser system (Z/Beamlet) came from the National Ignition Facility (NIF) prototype Beamlet laser, which was built and operated at LLNL starting in 1993 and shut down after successfully demonstrating its design goals in 1998.

Numerous modifications and upgrades to LLNL's Beamlet have been made to meet Sandia's requirements for Z/Beamlet laser, and to take advantage of advances achieved in the development of NIF technology. These include construction of a new fiber-

optic seed pulse generator (SPG) for the master oscillator room, with a picket fence pulse generator for pulse shaping. The pulse train shown in Figure 1 below was measured at the output of the Z/Beamlet regenerative amplifier earlier this year. When complete, the Z/Beamlet will produce up to 2 kJ of 0.53- μm laser energy in a picket fence of 2-ns total duration, with a final focus spot size 50 μm in diameter.

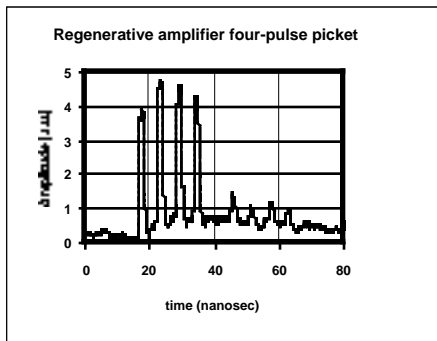


Figure 1. Picket fence laser pulse train generated by the new Z/Beamlet SPG and measured at the regenerative amplifier output. (Ralph Page)

Other major changes and modifications include: (1) upgrading the plasma electrode Pockels cell with NIF-style segmented anode and current return path; (2) changing the Beamlet amplifiers from 2x2 to a 1x2 aperture configuration, with commensurate savings in pulsed power requirements; (3) rebuilding the main cavity amplifiers with NIF-style blast-shield epoxy and side-loading the flashlamp cassettes; (4) reducing the main amplifier cavity length from 36 m to 30 m to fit in the available building space; (5) increasing the regenerative amplifier ring length to 28 ns for production of picket fence pulses up to 20 ns in overall duration. Several new optical systems have also been designed and constructed: (1) a new 1 and 2 output sensors and alignment systems; (2)

a new 2 relay telescope for the 75-m propagation from the frequency converter to the Z target chamber; (3) a new final focus optical system; (4) a new backlighter target alignment system; (5) a new calibration target chamber; (6) all control system computers have been replaced with Windows NT machines, and software has been updated as needed; and (7) the means have been provided for synchronizing Z/Beamlet shots with those of the Z facility within ± 250 ps.

In 1999, Sandia upgraded the 10,000-ft² Building 986 (adjacent to the Z facility) to Class 100,000 clean-room status with $\pm 1^\circ\text{F}$ temperature control to house the Z/Beamlet laser system. Installation of laser system components began in October 1999. A recent photograph of the Z/Beamlet high bay (Figure 2 below) shows the reassembled front end of the laser as well as part of the new cavity spatial filter. Main amplifier gain tests are expected to begin in June 2000; the frequency converter system will be activated this summer; and shots to a calibration chamber will be fired before the end of fiscal year 2000. Construction of the Z/Beamlet laser at Sandia represents an important interlaboratory collaboration that allows new applications of LLNL's high-energy solid-state laser technology.



Figure 2. Z/Beamlet front end and cavity spatial filter components installed in Sandia's Building 986. (John Caird)



Ultrafast Picket Fence Shapes to Enhance NIF Frequency Conversion and Power Balance

The National Ignition Facility (NIF) ignition targets require a high-contrast UV drive pulse shape that varies from a very low power foot at the beginning of the pulse to high peak power near the end. NIF currently converts 1 to 3 very efficiently (>80%) for high intensities at the peak, but less efficiently (<15%) during the foot. As a result, the net energy conversion for an ignition pulse is typically only ~50%. We have recently developed a new scheme for NIF pulse shaping which will increase the available 3 energy by ~40% and improve the power balance among beams by more than a factor of two. The increased energy makes possible new NIF target designs that could have yields exceeding a few 100 MJ.

The picket fence scheme replaces the continuous low-power foot with a sequence of shorter high-intensity "pickets." When averaged over the foot, the pickets supply the requisite low power, yet frequency convert efficiently. However, such schemes had previously been abandoned because the target is not illuminated for long durations between the picket pulses, which adversely affects the target performance. We have extended this concept to the sub-nanosecond regime, where pickets of duration of ~5 to 100 ps are separated by only a few 100 ps. With such a short interval between pickets, we can ensure that the target actually sees continuous illumination. A proposed implementation of this scheme for NIF

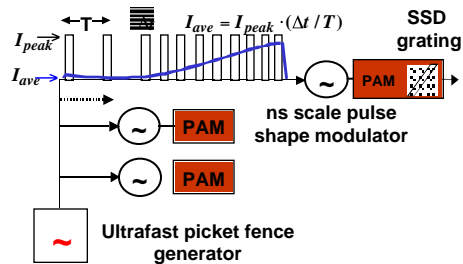
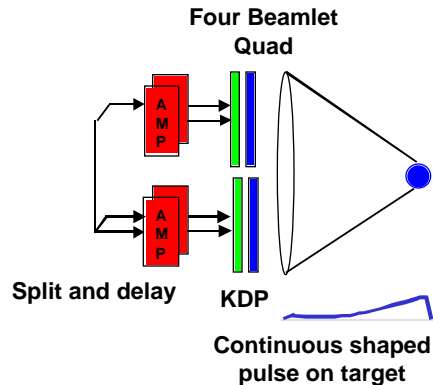


Figure 1: Schematic of proposed ultrafast picket scheme implementation on NIF. A single ultrafast picket generator is used as a source for all the NIF beamlines via 48 preamplifier modules.



(Fig. 1) has the advantage that it only requires the addition of a single modulator box in the master oscillator room. Continuous illumination is achieved by first temporally broadening the pickets at focus by the delay (~60 ps) imposed by the smoothing by spectral dispersion (SSD) grating. In addition, applying a ~60-ps delay sequentially within each of the commonly focused four beamlets of a quad ensures continuous illumination at focus for as much as ~250 ps between pickets.

The limit on how short the picket pulses can be is set by the bandwidth of frequency conversion. This limit is further compounded by self-phase modulation during propagation through the high-power amplifier. Calculation of the efficiency achieved with pickets as short as 20 ps shows that, in spite of the limitations, one sees a large improvement in conversion during the foot (from ~15% to 50%). The resulting net conversion efficiency of 3 energy to target is improved from ~50% to ~70%.

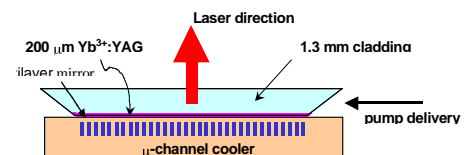
An unexpected benefit of this scheme is vastly improved power balance at 3. The conversion efficiency of the pickets saturates at much lower intensity owing to the aforementioned bandwidth and nonlinear effects. As a result, in the foot the 1 imbalance that is normally increased by a factor of ~3 upon conversion to 3 can instead be reduced upon conversion. A calculation of the resulting effect on the 3 power balance (Fig. 2) shows a large improvement. Thus, this scheme also provides a large margin for the challenging NIF power balance specifications, and is an attractive method to achieve the ~4% balance required for direct drive.

—Josh Rothenberg

First Light Generated from Yb:YAG/YAG Composite Thin-Disk Laser

We are working on a composite thin-disk laser that can be scaled to high brightness and high power for tactical weapons and other high-average-power applications. The key optical component is a diffusion-bonded composite comprised of a thin gain medium and thicker cladding that is robust and can be operated under high-average-power laser conditions. In contrast to high-power rod or slab lasers, a thin-disk laser with one-dimensional cooling geometry can be scaled gracefully to very high average power.

We have successfully demonstrated "first laser light" from thin-disk laser in the lab. During this experiment, optical pumping of the 1.5-mm-thick composite Yb:YAG/YAG laser element is achieved using a radiance-conditioned laser diode array and a lens duct. The gain medium is 200 μm thick and thermally contacted with 4 μm of indium solder to a cooler. We have achieved a laser power of 260 W at low duty factor and have used this data to anchor our laser modeling codes. The Yb:YAG/YAG composite gain element was fabricated by Onyx optics using diffusion bonding. Strong excitation and cooling of the thin laser gain medium was demonstrated and found to be consistent with our ray-trace model predictions. The efficacy of the heat removal using our first-generation cooler was tested by the prototype. Calorimetric data (coolant flow rate and temperature rise) under continuous diode pumping showed that we reached a heat dissipation rate of 1.1 kW/cm² at the surface of the cooler. The maximum heat flux attained was very close to that predicted in our design calculations. Based on our understanding of the thin-slab design, we believe that multi-kilowatt output can be achieved from a single thin-disk



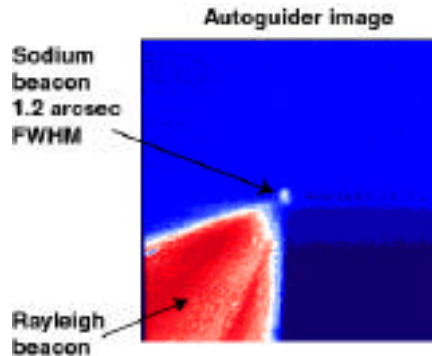
—Luis Zapata



Laser Guide Star (LGS) Systems at Lick and Keck Observatories

Adaptive optics have revolutionized optical astronomy over the last few years. These systems perform real time compensation of image distortions caused by atmospheric turbulence by sensing the distortions and correcting them. Typically, bright natural stars serve as reference beacons for the adaptive optics to sense the distortions, but, unfortunately, less than 1% of the sky has natural stars bright enough to use for correction. Under the support of LDRD and UC Relations Program, we are working with the Information Science and Technology Program to develop a fieldable sodium-layer LGS system for use on large astronomical telescopes in the Keck Observatory. Using an LGS at 589 nm, artificial stars can be created in the direction of observation by laser-induced fluorescence in the mesospheric sodium layer, 90 km above the earth's surface. Using LGS beacons enables the collection of diffraction limited images over 60% of the sky.

In 1992, an LGS feasibility demonstration was performed at LLNL, propagating 1100 watts from the AVLIS laser chain into the sky to form a sodium guide star visible from the ground with the naked eye. In 1996, workers from AVLIS program (Herbert Friedman, et al) installed a 20 W version of this laser, equipped with 127 elements adaptive optics, at the Lick Observatory on Mt. Hamilton, California and achieved significant image improvement on the 3-m Shane telescope. This system, using four pulsed, frequency-doubled Nd:YAG lasers to pump a dye master amplifier, preamplifier, and amplifier, produces up to 20 W at 11 kHz. The Lick AO/LGS system is now performing near theoretical limits, achieving a Strehl ratio as high as 0.4. A recent image of the sodium beacon on the sky, along with the Rayleigh scattered light from aerosol scattering in the lower atmosphere, is shown in the following photo. Recent improvements to the LGS system have dramatically improved the beam quality and system performance. The focus of the Lick LGS project is support of science observations and improving the LGS system for routine use.



A similar AVLIS laser system was delivered to the Keck Observatory in Hawaii for use on one of the twin 10-m telescopes. This was installed at Keck headquarters in Waimea, Hawaii in 1998, prior to full completion of the laser system. Numerous modifications and upgrades to the earlier LGS design have now been made to meet the evolving requirements for a reliable, robust, and remotely operable system, allowing safe operation at 14,000 ft. Among the changes made were the installation of safety interlocks and diagnostics to prevent optical damage to the system. We redesigned the relay optics to reduce hard edge diffraction in the dye laser, while optimizing power and beam quality. Motorized waveplates with polarizers in the YAGs allow remote power balancing between amplifier pump beams. This significantly reduces the jitter of beam pointing. To extend the lifetime of frequency doubling of the YAG lasers, we replaced KTP with LBO crystals. Automated startup and shutdown sequencing has also significantly reduced the rate of damage in the system.

Several 8-hr/day laser runs have been performed at Keck (see photo) and have demonstrated excellent stability and beam quality. A run in June demonstrated an average power of 14.8 W with 1.5% energy stability and a Strehl ratio of 0.647. In addition, a 5 day, 8 hr. per day operations test was just completed, demonstrating the improved reliability of the system. The Keck LGS modifications should be complete later this year. Planning for the move to the summit of Mauna Kea will begin in August

with system deployment on the Keck II telescope expected by early 2001. The Keck LGS uses frequency-doubled Nd:Yag laser as its pump source. The dye oscillator and pump lasers will be installed on the floor of the telescope dome and will be fiber-optically coupled to the dye amplifiers mounted on the elevation ring of the telescope.



A recent Decadal Review by the National Academy of Sciences identified the construction of a large-aperture telescope as the highest priority for ground-based astronomy in the next decade. The California Extremely Large Telescope (CELT) is a 30-m telescope proposed for construction by 2010, as a collaboration between U. C. and Caltech. The capability to use multiple laser guide stars routinely was identified as the primary key enabling technology for these next generation telescopes. Multiple lasers guide stars will be required to compensate for turbulence across the increased telescope aperture. As a result, it is clear that development of a compact, robust, reliable solid-state guide star laser technology is required. This year we received funding to identify the most promising laser technology for further development. The design we selected is based on sum-frequency mixing of two fiber lasers in a periodically poled crystal to produce a 10 W, CW beam at 589 nm. Technology demonstrations will begin in FY01.

(Dee Pennington)

Laser Peening Reduces Stress-Induced Corrosion and Cracking of Welds

In a joint research effort with the Yucca Mountain Project (YMP), we are evaluating laser peening as a technique to improve the corrosion resistance and lifetime of welds in alloy 22. Nuclear waste from nuclear reactors around the country will be stored underground at Yucca Mountain in welded containers of Alloy 22. These containers are required to last 10,000 years without leakage. However, the process of welding the end caps on these containers can cause tensile stress that allows defects to grow into cracks and accelerate corrosion. Previous work has demonstrated that laser peening can transform tensile stress into compressive stress deep into the material and prevent the growth of such cracks. We have found that our high-energy, phase-conjugated Nd:glass zigzag slab lasers are ideal for laser peening due to their very uniform transverse mode profile and their adjustable pulse width.

The process of stress-corrosion cracking (SCC) can be greatly accelerated using an aqueous solution of $MgCl_2$ at a temperature greater than 120° C. To maintain a constant temperature, the solution is saturated and kept in a closed glass vessel. The samples are suspended in the solution using Teflon tape and are removed and examined every two to four hours for signs of cracking.

To date, we have conducted a number of SCC proof-of-principle experiments for YMP. The first of these experiments was on a seam-weld of two pieces of 3 mm x 18 mm x 75 mm 304 stainless steel. One of the welds was laser peened and the other weld was not. The unpeened sample showed cracks within 24 hours, while the laser-peened sample showed no signs of cracking or corrosion after seven days! More recently, we have conducted similar tests with U-bends of 304 stainless steel. The U-bends are a more severe test because of the much higher stress. The unpeened U-bends broke into two pieces within two hours, while the laser-peened U-bends showed no signs of cracking after more than six days! The results from this experiment are shown in the following figure.



U-bends in 304 stainless steel after SCC tests performed by F. Wang.

(John Honig)

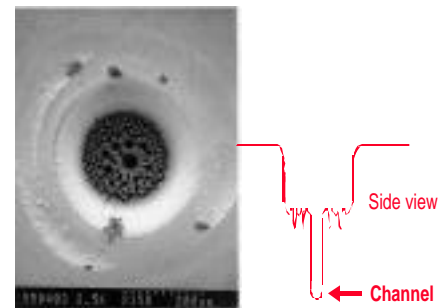
Interesting Phenomena in Short-Pulse Laser Machining

The use of sub-picosecond laser pulses for drilling, cutting, and film deposition has proven to produce high-quality features (e.g., no heat-affected zone and precise control of feature shape) in a wide variety of materials. Because of the high intensity ($>10^{12}$ W/cm²) and short pulse, energy is absorbed in a thin layer and material is removed before the absorbed energy can be transferred to the surrounding bulk material. Several and work-for-others contracts have been initiated at Lawrence Livermore National Laboratory because of the potential advantages for commercial applications. The High Explosives Applications Facility (HEAF) has taken delivery on a 5-W "portable" laser system for use in experiments with energetic materials because of the demonstrated capability for machining without heat.

However, the ablation process using ultrashort laser pulses has proven to be more complex than originally thought. We have observed instabilities that lead to a high degree of surface roughness at the bottom of a hole above a certain fluence. This is illustrated in the figure in the next column that shows the bottom of a blind hole drilled in stainless steel at 10 J/cm². Not only do many small circular holes with connecting channels form, but a central channel (30 – 70 μm in diameter) forms near the peak of the incident laser fluence.

There is no apparent correlation between the size and position of these subholes and the nonuniformity in the incident laser beam. Nonetheless, shaping the incident radiation such that the peak fluence is a ring around the edge of the beam results in a ring of channels around the edge of the hole bottom. This behavior is also influenced by the material that is being ablated; for example, these deep channels were not observed in copper up to fluence of 15 J/cm².

For stainless steel and aluminum, the average ablation rate does not increase significantly with fluence above 0.5 J/cm². If we measure the depth of the flat bottom after several thousand shots, a constant drilling rate was observed (about 20 nm per pulse for stainless steel and 80 nm per pulse for aluminum). However, if we measure the depth of the deepest point in the hole, the drilling rate per pulse appears to increase with laser fluence. For stainless steel and aluminum, the bottom becomes rougher above approximately 1 J/cm² until the channel mentioned above forms at about 5 J/cm². At this point, the rate at which this channel is drilled increases dramatically with fluence. This dramatic increase in drilling rate with fluence is not seen in copper. Finally, we observed that the overall ablation rate for aluminum and copper is 4–5 times that of stainless steel. The material properties that influence this have not yet been determined.



Scanning electron micrograph of hole drilled for 6000 shots with a Gaussian spatial profile at normal incidence in stainless steel, 1-ps pulse length, circular polarization, 10 J/cm². The inset is a rough depiction of how the crosssection would look.

(Paul Banks)



Laser Science & Technology

Dr. Howard T. Powell, Program Leader

UCRL-TB-136126-00-09

Fabrication of 160-kW Diode-Laser Arrays Now Completed

We have completed a 160-kW peak-power diode array for use in pumping the Yb:S-FAP slabs that serve as the gain medium in the Mercury laser. This diode array uses a low-cost packaging technology developed at LLNL for moderate duty factor application. In our approach, diode submounts or tiles are fabricated using a silicon etching technology. These tiles serve to precisely position and hold 23 laser diode bars. The precision positioning that is enabled by the silicon submount allows the use of high-precision cylindrical microlenses to be located in front of each diode bar as shown in Figure 1 below. The lenses, which collimate the highly divergent "fast-axis" diode radiation, are critical for the production of high-radiance pump beams that will be used to excite laser crystals at high irradiances. With each bar typically being able to generate in excess of 100 W of peak power, an individual tile is capable of sourcing in excess of 2.3 kW of pump radiation. Large pump arrays are built up by juxtaposing individual diode tiles.

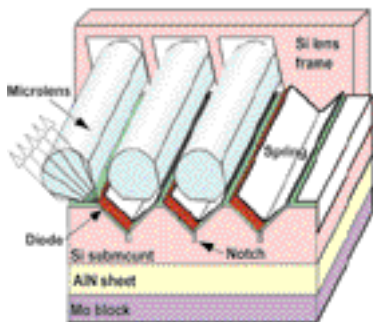


Figure 1. LLNL-developed low-cost diode laser submount uses silicon etching technologies to fabricate a structure that can precisely hold 23 diode bars on an individual tile.

On an individual tile the diode bars are electrically connected in series. A typical current pulse to the tiles will have up to a 1-ms duration and a peak amplitude of 140 amps. Figure 2 shows the optical output power of one tile as a function of the drive current peak amplitude. The peak optical output power from the array is 2.75 kW and incorporates an almost 20% safety margin over the performance level.

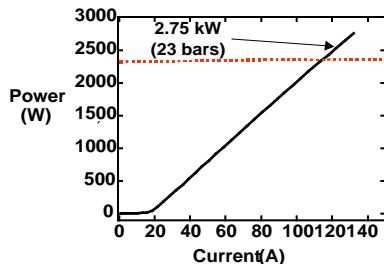


Figure 2. Output optical power from a single 23-bar tile as a function of the drive current applied to the tile. The red line indicates the minimum acceptable level for the Mercury laser.

The Mercury laser will utilize four groups of tiles, each group referred to as a backplane array, which will be used to end-pump the Yb:S-FAP laser slabs. Each of the four backplanes will consist of 72 individual tiles. We have completed fabrication of the tiles for one of the backplanes, which will generate in excess of 160 kW of peak optical power and be used to perform preliminary experiments. Figure 3 below shows 42 of the 72 tiles that will be used in constructing the first Mercury backplane array.



Figure 3. Mercury laser backplane array. (Barry Freitas)

Deuterium Cluster Fusion Neutron Pulse Width Characterized

Last year we reported the first observation of nuclear fusion from the explosions of ultrafast laser-heated deuterium clusters. A picture of the apparatus used for laser irradiation experiment is shown in Figure 4. Since that initial experiment, the Falcon team has undertaken a series of experiments to characterize the phenomenon and to assess the

viability of this technique with a much higher average-power laser to yield useful, small-scale neutron sources for materials irradiation.

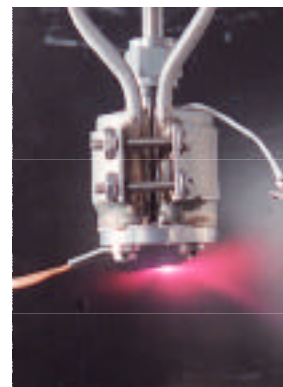


Figure 4. Falcon gas jet neutron source.

The most striking result has been the measurement of the neutron pulse duration. These measurements have shown that the emitted neutron pulse at the interaction point has duration of only a few hundred picoseconds (see Figure 5), consistent with fusion reactions in an inertially confined hot deuterium plasma. The spread in neutron pulse width with distance arises from the finite energy spread of the 2.45 MeV neutrons produced by the temperature of the reacting plasma (multi-keV).

This result is intriguing as it may ultimately enable a new class of experiments in which a short neutron pulse is used as a pump to trigger dynamics in a material that can then be probed as a function of time with a second optical or x-ray pulse.

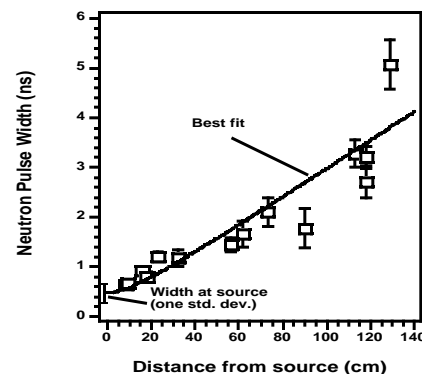


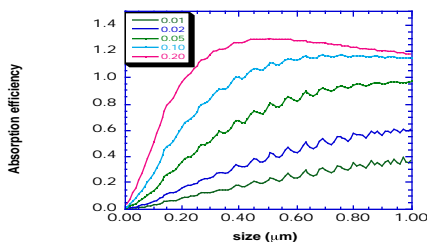
Figure 5. Measured neutron pulse width as a function of distance from the cluster plasma. (Todd Ditmire)

Modeling of Laser-Induced Damage in NIF UV Optics

Reducing laser-induced damage to UV optics in the National Ignition Facility's (NIF's) final optics assembly is important for reducing operational costs. Full NIF performance corresponds to 8 J/cm² of average fluence at 3-ns pulse lengths and at 351 nm in the optics downstream from the conversion crystals. Recent experimental and theoretical progress has led to reductions in the number of surface-damage initiators and in understanding the evolution of damaged-area growth upon multiple laser-pulse irradiation. Work is continuing to identify and eliminate surface-damage initiators that are operative in the 8–14 J/cm² fluence range. Since it is unlikely that all initiators can be removed, especially under operational conditions, it remains important to understand how damaged areas grow upon repeated irradiation and to determine the factors that most influence growth. LS&T has contributed to a broad modeling effort to investigate physical mechanisms underlying observed damage behavior and to aid in the design and interpretation of experiments.

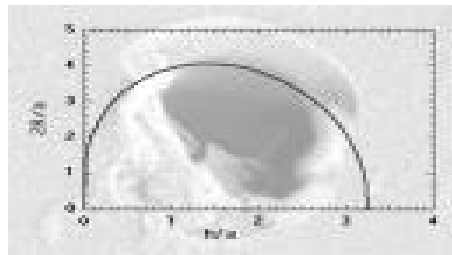
Initial laser damage in nominally transparent materials can be due to extrinsic factors like absorbing contaminants. We are investigating the energy absorption by such contaminants and the resultant damage craters in order to help identify initiators. Typical initiation craters range in size from a few microns to a few tens of microns in size.

The role played by microcracks created by surface finishing is of particular interest for damage growth. Two ways such cracks can be important are through local electric field intensification due to total internal reflection and through trapping light-absorbing contaminants. Cracks can also exhibit absorbing electronic surface states that can be potential initiators.



We performed a series of Mie scattering calculations to determine the absorbed fraction of laser energy incident on the geometric cross section of small absorbing particles in silica. The curves in the figure in the first column were generated for various values of the imaginary part of refractive indexes. This fraction can be larger than 100% due to diffraction. The strongest absorption shown corresponds to ceria contaminants corresponding to an imaginary refractive index value of 0.2.

The theoretical curve shown below describes the relationship between crater diameter $2R$ and depth h beneath the surface of absorber of radius a . Our observed initiation craters correspond



to the shallow end of this curve implying that the defects are near the surface.

We have also begun simulations of field intensification in the vicinity of typical crack networks and evaluation of its importance for both damage initiation and subsequent growth. Absorption and intensification simulations together with detailed numerical simulations of crater formation will enable development of a comprehensive model of laser damage including both damage initiation and growth.

(Mike Feit)

4th Harmonic Laser Trigger System for the Z Accelerator

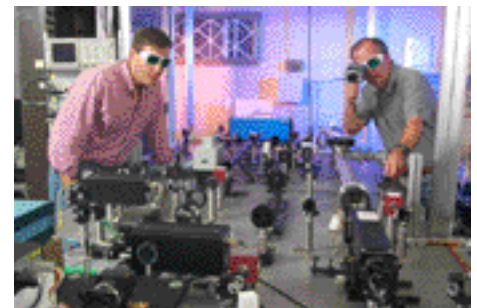
Under sponsorship of Sandia National Laboratories, we have designed, built, and tested a Nd³⁺ laser that produces near diffraction-limited, high-energy laser pulses at the 4th harmonically converted wavelength of 263 nm. The objective of this laser system is to initiate breakdown in Z accelerator's high-voltage switches. The switches deliver currents of several megamperes to dense electric discharges, called z pinches, which generate

intense x rays used to drive inertial confinement fusion (ICF) and other high energy density physics experiment for DOE's Stockpile Stewardship Program.

The solid-state laser we have built offers several advantages relative to the 248-nm KrF excimer laser currently used to trigger the Z accelerator's high-voltage switches. Chief among these is superior beam quality and shorter pulse rise time (several hundred ps), properties expected to reduce switch timing jitter and improve synchronization of the Z accelerator with its diagnostic x-ray backlighter pulse. The backlighter pulse will be generated by Z/Beamlet, a 2-kJ, 526-nm laser now being constructed by a joint LLNL–Sandia team. Such backlighter pulses generate point sources of x rays for generating time-resolved radiographs of imploding ICF targets on other target packages. Backlighter beams have been used in other ICF facilities.

The trigger laser, shown below, effectively generates pulses at 1,053 nm using an injection-seeded Nd:YLF regenerative amplifier and a 4-pass 1-cm Nd:glass rod amplifier. A phase conjugator is used to maintain 2–3 times diffraction-limited wavefront quality. The 10-ns output from the four-pass amplifier feeds three separate channels, each with a single-pass 1-cm rod amplifier and a pair of BBO crystals for frequency conversion to the fourth harmonic. We have recently completed testing on one of these channels and obtained ~850 mJ at 263 nm with 3.6-J incident radiation at 1,053 nm. A harmonic conversion efficiency of >25% was achieved as limited by two-photon absorption at 263 nm. The laser is slated to be activated at Sandia's Z accelerator in Albuquerque, NM, in 2001.

(A. Erlandson)



Thin Glass Sheets as Disposable Debris Shields on NIF

On the National Ignition Facility (NIF), considerable amount of debris will be generated when the 192 laser beams irradiate the inertial confinement fusion (ICF) and other experimental targets. The debris consists of various-sized particles ranging from atomic vapor to ~millimeter-sized shrapnel. Small-sized debris can coat the debris shield while larger-sized shrapnel can produce pits in the debris shield. Both mechanisms lead to increased optical damage of the debris shield on subsequent laser shots and consequently shorten its service life. This could significantly increase the operating cost of NIF. One approach to resolve this issue consists of protecting each main debris shield on NIF using a thin glass sheet as a disposable debris shield (DDS). Such sheets would have to be changed on each laser shot. For this method to be practical, the glass sheets would have to be inexpensive and have acceptable wavefront and transmission characteristics.

We have recently identified a thin glass sheet material for this application. The glass sheets can be manufactured with thickness as thin as 50 μm with good optical quality. They were developed originally for use as screens on flat-panel displays. Figure 1 shows one of such thin sheets produced by Corning.

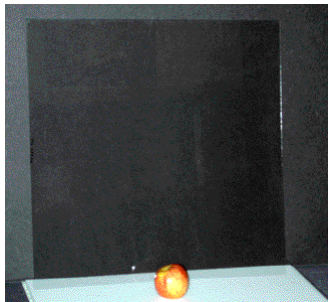


Figure 1. A 440x440-mm-size, 0.7-mm-thick glass sheet.

We have acquired such sheets from several vendors for evaluation purposes. The glass sheets are made either through extrusion, fusion bonding, or a float process. Generally, the extrusion-drawn glass sheets tend to exhibit large thickness variations orthogonal to the draw direction and very small variations along the draw direction. The measured wavefront of one such sheet, shown in Figure 2, illustrates this point.

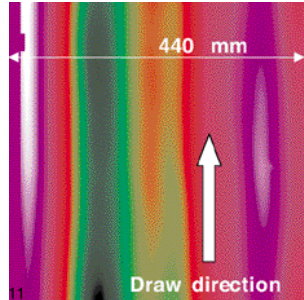
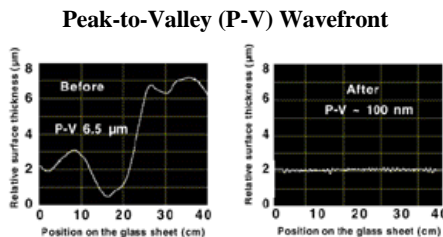


Figure 2. Phase map of a 0.7-mm-thick glass sheet. Peak-to-valley surface thickness variation is about 8.5 μm.

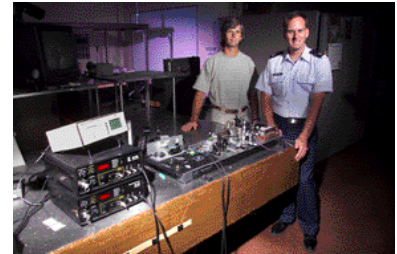
Float glass sheets tend to have more two-dimensional thickness variation. When such thin sheets are used as DDS, the focal spot on NIF is degraded due to the additional phase aberrations of the thin glass sheets. We are currently evaluating the feasibility of using such sheets on NIF.

We successfully developed a wet etch tool to improve the flatness of thin glass sheets for NIF and for the Eyeglass project. An example of the improvement of the wavefront after the processing is shown in the graphs below. Numerical simulations suggest that the removal of the one-dimensional thickness variations is quite adequate for ICF spot sizes. Another way to accommodate the DDS aberrations is by “tightening” the continuous phase plate spot to allow for its enlargement due to DDS aberrations.

The acceptability of this DDS concept is currently under evaluation from the target physics perspective. In parallel, we are also assessing the survivability of these debris shields under the shrapnel impact as well as their response to high-power NIF pulse irradiation.



(S. Dixit & P. Whitman)



1100-nm Yb:Fiber Laser Delivered to the Air Force Research Lab

Under sponsorship of the Air Force Research Laboratory (AFRL), we have designed, built, and tested a Yb:fiber laser that produces single-line and single-mode 2-W output power at 1100 nm. This very bright source will be fed to a more powerful amplifier at the AFRL, located at Kirtland Air Force base. Capt. Nathan Brilliant completed this work at Lawrence Livermore National Laboratory in conjunction with colleagues from Laser Science & Technology.

The oscillator is a standard 1100-nm fiber laser manufactured by Ionas of Denmark, which we spliced to a fiber isolator and wavelength division multiplexer to seed a preamplifier. The output power of the preamplifier is 43 mW with a slope efficiency of 33%. The output from the preamplifier is again spliced to a fiber-coupler, collimated through a “free space” isolator and then propagated to seed to a double-clad amplifier. The double-clad fiber, made by Polaroid, is 10 meters long with an 8-μm-diameter doped core and 165-μm hexagonal pump cladding. The seed and pump beams are counterpropagated in the amplifier to prevent early saturation. A fiber-coupled diode laser was used to pump the double-clad fiber amplifier. Since the pump beam is trapped in the pump cladding, it crosses the ytterbium-doped core many times and is absorbed along the 10-meter length. We successfully achieved an optical-to-optical efficiency of 28%.

Although this laser does not operate at the wavelength commonly used in telecommunications, it can be fabricated using fiber-optic components developed for optical communication. We are exploring other possible applications, including laser guide stars, for this single-mode fiber laser.

(Capt. N. Brilliant & A. Drobshoff)

The HELSTF Heat-Capacity Laser Successfully Demonstrates 10-kW Output

Under the support of the U.S. Army's Space and Missile Defense Command, and in collaboration with industrial partners (Raytheon, Litton Airtron, and others), we are developing high-average-power (100-kW class), diode-pumped solid-state, heat-capacity laser technology for applications in tactical short-range air defense missions. The ultimate vision is an electrically powered, diode-pumped, solid-state weapon that can be deployed on a hybrid electric vehicle. To establish a solid technical basis for the heat-capacity laser operation and risk reduction, we built a flashlamp-pumped Nd:glass laser prototype. In earlier work, a 3-disk heat-capacity laser amplifier module was successfully operated at 10 Hz with an output of 140 J/pulse. We have recently completed construction of a 10-kW prototype (9-disk Nd:glass amplifier pumped by flashlamps) to be installed in the Army's High Energy Laser Strategic Test Facility (HELSTF). The photo below shows the 9-disk heat-capacity amplifier under testing.



This 9-disk module is designed to have 10-kW average output power and deliver laser pulses with beam quality $<3\times$ diffraction-limited and energy of 500 J/pulse at 20 Hz for 10-second bursts. The laser amplifier is now fully operational for pulse repetition operation using testbed power supplies.

During the past month, the 9-slab amplifier was operated using a stable resonator with an output coupling of 29%. In the initial testing

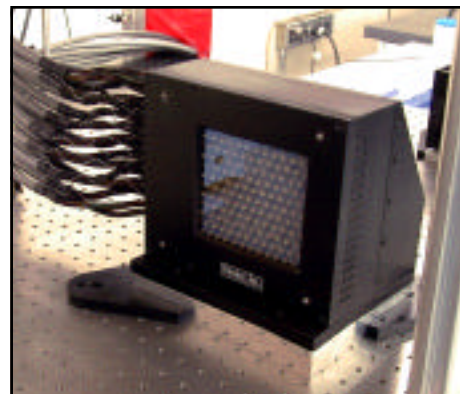
we successfully achieved an output power exceeding 10 kW for a burst of 100 pulses. The average pulse energy was 558 J with a pulse repetition frequency of 18.5 Hz. Experiments are also under way to measure gain uniformity and wavefront distortion to characterize a deformable mirror system to meet system requirements delineated to the HELSTF.

Using the 9-disk prototype heat-capacity laser described above, we performed a series of target interaction experiments. Metal coupons were irradiated by the high-energy laser beam. During these tests, the heat-capacity laser was operated at 3 Hz with energy of 650 J per pulse. The irradiation pulse has a temporal envelope of 300 to 400 microseconds and consists of several relaxation-oscillation spikes with peak intensities near MW/cm^2 . The laser beam was configured to a 6×6.5 mm rectangular spot onto the target. To guide future target interaction experiments, we continue to develop numerical models to simulate the material removal process using hydrodynamics codes to model the vaporization and material ejection process.



The photo above shows preliminary material removal tests made with the 9-disk module. The protective window transmission had dropped to 50% by the end of this initial run due to molten aluminum deposition. In parallel with laser amplifier activation, work on the adaptive resonator is also making good progress. Components for the adaptive resonator, such as deformable mirror (DM), DM control electronics, and laser diagnostics sensor packages, have been assembled, and characterization tests are under way. Full-

power operation of the 9-slab amplifier with the adaptive resonator is expected early 2001.



The development of a diode-pumped Nd:GGG heat-capacity amplifier testbed is proceeding in parallel. We have made significant progress toward the growth of high-quality Nd:GGG boules. Litton Airtron SYNOPTICS is now routinely growing 10 to 15 cm of Nd:GGG with high optical quality. We have also completed the design and testing of a new SiMM (silicon microchannel monolithic) heatsink package for high-power laser-diode arrays and successfully demonstrated output irradiance of $1 \text{ kW}/\text{cm}^2$ from a 10-bar diode array, as required. Using a large-area diode array as pumping source, we completed emission cross-section and thermal deposition measurement on Nd:GGG. It appears that Nd:GGG will provide the higher extraction efficiency and fracture strength needed for a 500-J, 100- to 250-kW average power heat-capacity laser system.



(Brent Dane)